BIOCHEMISTRY
including biophysical chemistry & molecular biology
Article

Biochemistry **2010,** *49,* 4687–4694 4687
DOI: 10.1021/bi901612y

Structural Impact of Human and *Escherichia coli* Biotin Carboxyl Carrier Proteins on Biotin Attachment†

Shannon Healy,*,‡ Megan K. McDonald,‡ Xuchu Wu,‡ Wyatt W. Yue,§ Grazyna Kochan,§ Udo Oppermann,§ and Roy A. Gravel‡

‡*Department of Biochemistry and Molecular Biology, University of Calgary, Calgary, Alberta, Canada T2N 4N1, and* §*Structural Genomics Consortium, University of Oxford, Oxford, U.K.*

Received September 15, 2009; Revised Manuscript Received May 1, 2010

ABSTRACT: Holocarboxylase synthetase (HCS, human) and BirA (*Escherichia coli*) are biotin protein ligases that catalyze the ATP-dependent attachment of biotin to apocarboxylases. Biotin attachment occurs on a highly conserved lysine residue within a consensus sequence (Ala/Val-Met-Lys-Met) that is found in carboxylases in most organisms. Numerous studies have indicated that HCS and BirA, as well as biotin protein ligases from other organisms, can attach biotin to apocarboxylases from different organisms, indicating that the mechanism of biotin attachment is well conserved. In this study, we examined the cross-reactivity of biotin attachment between human and bacterial biotin ligases by comparing biotinylation of p-67 and BCCP87, the biotin-attachment domain fragments from human propionyl-CoA carboxylase and *E. coli* acetyl-CoA carboxylase, respectively. While BirA has similar biotinylation activity toward the two substrates, HCS has reduced activity toward bacterial BCCP87 relative to its native substrate, p-67. The crystal structure of a digested form of p-67, spanning a sequence that contains a seven-residue protruding thumb loop in BCCP87, revealed the absence of a similar structure in the human peptide. Significantly, an engineered "thumbless" bacterial BCCP87 could be biotinylated by HCS, with substrate affinity restored to near normal. This study suggests that the thumb loop found in bacterial carboxylases interferes with optimal interaction with the mammalian biotin protein ligase. While the function of the thumb loop remains unknown, these results indicate a constraint on specificity of the bacterial substrate for biotin attachment that is not itself a feature of BirA.

Propionyl-CoA carboxylase (PCC)[1] is a mitochondrial enzyme involved in the catabolism of branched chain amino acids, odd-chain fatty acids, and cholesterol. PCC is made up of two non-identical subunits, the α subunit consisting of a biotin carboxylase (BC) domain at the amino terminus and a biotin carboxyl carrier (BCC) domain at the carboxyl terminus, and the *β* subunit containing the carboxyl transferase (CT) domain (*1*−*3*). Biotin is attached to a lysine residue within the consensus tetrapeptide Ala/Val-Met-Lys-Met in the BCC domain, which is nearly universally conserved in biotin-dependent carboxylases from bacteria to humans (*4*). Biotin attachment is catalyzed by a biotin protein ligase (BPL), called holocarboxylase synthetase (HCS) in humans (*5*) and BirA in *Escherichia coli* (*6*). Truncated forms of BCC domains that retain the capacity to be biotinylated by BPLs have defined the minimum size for biotinylation to be 67−87 residues, with the biotin-attachment site in the center (*7*−*10*). These criteria were applied to generate p-67, which is the C-terminal 67 amino acid BCC domain of the PCC α subunit (*7*). Similarly, BCCP87 corresponds to the C-terminal 87 amino acid BCC subunit from *E. coli* ACC (*8*).

The structure of the apo (unbiotinylated) form of BCCP87 has been solved by NMR spectroscopy (*11*) and the holo (biotinylated) form by X-ray crystallography using subtilisin digestion of full-length holo-BCCP (*12*). Both forms appear to be structurally identical, indicating that the addition of biotin does not result in a significant conformational change. The structure is that of two four-stranded antiparallel *β*-sheets that pack together to form a *β*-sandwich fold (Figure 1). The hydrophobic core is lined with conserved glycine and hydrophobic residues that destabilize the domain and impair biotinylation when mutated (*7*, *13*). The two symmetric halves of the protein are divided by a *β*-hairpin loop which, at the end of the *β*-hairpin turn, is the site of biotin attachment (*4*). A second nine residue "protruding thumb loop" (Thr94−Phe102) resides between *β*-strands 2 and 3. The structures of numerous other biotin-attachment domains from bacteria and archaebacteria have been solved (*11*, *12*, *14*, *15*), including the structure of human pyruvate carboxylase (PC, lacking the N-terminal BC domain) (*16*) and the BCC domain of human acetyl-CoA carboxylase 2 (ACC-2) (*17*). The overall protein fold of all known biotin-attachment domains is well conserved (Figure 1). However, among the structures currently solved, the protruding thumb loop is present only in BCCP87.

Characteristically, biotin protein ligases show biotinylation activity toward different apocarboxylases from diverse organisms (*4*, *7*). The functional interaction between biotin protein ligases and carboxylases is therefore predicted to be highly conserved in all organisms. There has been some indication, however, that

†These studies were supported by a Canadian Institute for Health Research grant to R.A.G. and scholarship support to S.H. from the CIHR Strategic Training Program in Genetics, Child Development and Health, at the University of Calgary.

*Address correspondence to this author at the Department of Signal Processing, Tampere University of Technology, Tampere, Finland FI-33720. Telephone: (0) +358331153928. Fax: (0) +358331154989. E-mail: shannon.healy@tut.fi.

[1]Abbreviations: HCS, holocarboxylase synthetase; BCCP, biotin carboxyl carrier protein; PCC, propionyl-CoA carboxylase; BPL, biotin protein ligase; TEV, tobacco etch virus; MALDI-MS, matrix-assisted laser desorption/ionization mass spectrometry; ACC, acetyl-CoA carboxylase; PC, pyruvate carboxylase.

Published on Web 05/05/2010

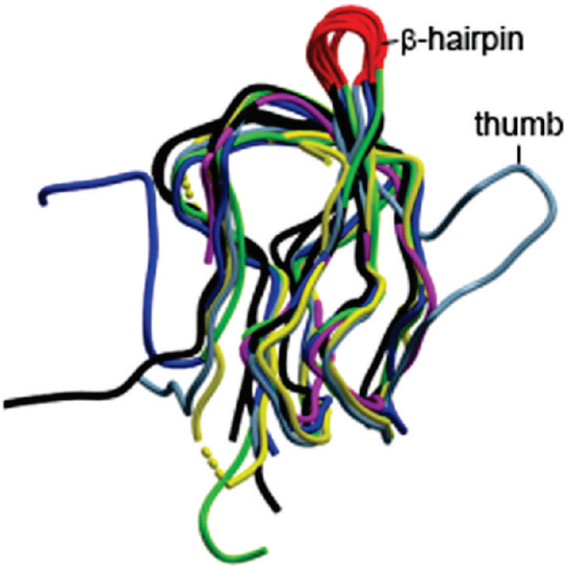

FIGURE 1: Structural conservation of the BCC domain. C^{α} backbones from various BCC domain structures were superimposed to demonstrate the high level of conservation across species. The biotin-attachment consensus sequence (Ala/Val-Met-Lys-Met) on the β-hairpin loop is colored in red. The thumb loop in *E. coli* BCCP-87 is indicated. The structures of *R. etli* PC (yellow, PDB code 2QF7), *B. subtilis* BCCP (green, PDB code 1Z7T), *E. coli* BCCP87 (gray, PDB code 1BDO), *P. shermanii* transcarboxylase (blue, PDB code 1DCZ), human ACC-2 (purple, PDB code 2DN8), and *P. horikoshii* BCCP (black, PDB code 2EVB) are included. Structural manipulations were conducted using MolSoft ICM-Browser (La Jolla, CA).

biotin protein ligases have a higher activity toward their own natural substrate. One study compared the activity of yeast biotin protein ligase (yBPL) and *E. coli* BirA toward the truncated BCC domain of yeast pyruvate carboxylase (yPC-104) and *E. coli* BCCP87 (*18*). The K_M of both yPC-104 and BCCP87 were found to be increased by 10-fold when incubated with BirA or yBPL, respectively, relative to their natural BPL. The authors used homology modeling, with the known structure of BCCP87 (*11*) as a template, to predict the structure of yPC-104. While the two biotin-attachment domains were structurally very similar, the protruding thumb loop present in BCCP87 was not found in yPC-104. This structural difference between BCCP87 and yPC-104 was predicted to contribute to the change in affinity.

In this study we compared biotin attachment by recombinant BirA (*E. coli*) and HCS (human) on p-67 and BCCP87. We found that while BirA has a similar rate of reaction toward the two biotin-acceptor domains, HCS has reduced reactivity toward BCCP87 compared to p-67. The results suggest that HCS was able to discriminate between native and non-native substrates. Structural analysis of p-67 using X-ray crystallography revealed absence of a protruding thumb loop in the human protein. With generation of a "thumbless" form of BCCP87, we found that HCS activity toward this substrate was partially restored with significantly improved substrate binding. Our findings suggest that HCS has evolved to selectively recognize and bind to unique structural elements in its native protein substrates.

MATERIALS AND METHODS

p-67 Protein Expression and Purification. The biotin-attachment domain of the PCC α subunit, p-67, comprising the C-terminal 67 residues of the polypeptide (Leu637−Glu703) with an attached N-terminal His tag, was expressed and purified as described previously (*19*). For optimal crystallization, p-67 was lengthened to include four upstream residues (Thr633−Glu 703) and subcloned into the pNIC28-Bsa4 vector (GenBank accession number EF198106), which fuses a 6×His tag with a TEV protease cleavage site on the N-terminal end of the protein. For clarity in this study, "p-67L" will be used to describe this longer version of the domain. The cDNA for p-67L was inserted in the vector using ligation-independent cloning and transformed into BL21(DE3) Rosetta cells. p-67L was expressed and purified as with p-67 and stored in 50 mM HEPES pH 7.5, and 100 mM NaCl. The tag was removed by TEV digestion, followed by brief mixing with 50 μL of Ni-agarose, which binds both His-tagged TEV and the cleaved His tag. The flow-through containing tag-removed p-67 was collected, and the resin was washed with 3 column volumes of 50 mM HEPES, pH 7.5, and 100 mM NaCl. The protein was concentrated to 21−48 mg/mL using an Amicon Ultra-15 concentrator with a 3 kDa cutoff (Millipore). The identity of p-67L was confirmed by ESI-ToF (expected, 9928.2 Da; observed, 9928.8 Da). Protein was stored at −80 °C.

"Thumbless" BCCP87 Protein Expression and Purification. Mutant BCCP87, lacking the thumb loop, was generated by replacement of the seven residues comprising the thumb loop (-Thr-Pro-Ser-Pro-Asp-Ala-Lys-) with a single alanine residue. The cDNA for this BCCP87 mutant, BCCP87ΔT, was generously provided by J. Cronan, University of Illinois (*20*). BCCP87ΔT was subcloned into the pNIC28-Bsa4 vector and purified with Ni resin as described above.

Preparation of HCS, BirA, and BCCP87. Biotin attachment to BCCP87, BCCP87ΔT, and p-67 was compared in a time-course study using HCS or BirA as the catalytic enzyme. BCCP87 was generously provided by D. Beckett, University of Maryland (*10*). Recombinant HCS was purified from a GST-fusion expression vector as described in a previous study (*19*).

Biotin Attachment Assays. Two methods were used to examine the rate of biotin attachment. The first method used autoradiography to detect biotin labeling on BCCP87, BCCP87ΔT, and p-67. The enzymatic reactions were prepared consisting of 1 μM HCS (final concentration), 100 μM p-67, BCCP87, or BCCP87ΔT, 100 μM [^{14}C]biotin, and 1 mM ATP brought to a total volume of 20 μL with 10 mM Tris-HCl (pH 7.5 at 20 °C), 200 mM KCl, and 2.5 mM $MgCl_2$. Assays were incubated for various durations at 20 and 37 °C. The reaction was stopped by adding 5 μL of SDS electrophoresis buffer with heating (95 °C/5 min). These samples were run on a 16.5% Tris−tricine discontinuous gel and dried in cellophane for direct exposure (4−5 days) to a phosphoimager screen. Bands were detected by scanning the phosphoimager screen on a Storm 860 phosphoimager scanner, followed by data manipulation and band density measurement using the software ImageQuant TLv2005.

A second method was used to define the kinetic parameters for HCS and BirA, by measuring incorporation of [^{3}H]biotin onto p-67, BCCP87, or BCCP87ΔT, as described by Chapman-Smith et al., with modifications (*13*). In brief, the reactions contained 10 mM Tris-HCl (pH 7.5 at 20 °C), 200 mM KCl, 2.5 mM $MgCl_2$, 5 μM biotin, 4.5 pmol of [^{3}H]biotin (specific activity 35−44 Ci/mmol; Perkin-Elmer), 14 nM HCS or BirA, and an increasing amount (1.25−150 μM) of p-67, BCCP87, or BCCP87ΔT, to a total volume of 100 μL. The reaction was initiated by adding HCS or BirA and incubated at 37 °C for 30 min unless otherwise stated. Twenty microliter aliquots were spotted onto biotin and trichloroacetic acid-treated filter paper and dried. The filter papers were washed twice in 10% ice-cold trichloroacetic acid,

Table 1: Crystallographic Data Collection and Refinement Statistics of p-67L

PDB code	2JKU
Data Collection	
space group	$P6_422$
unit cell parameters	
a, b, c (Å)	56.11, 56.11, 58.08
γ (deg)	120
resolution range (Å)	48.56−1.50 (1.60−1.50)
redundancy	12.7 (13.4)
completeness (%)	99.9 (100.0)
$\langle I/\sigma(I)\rangle$	23.6 (5.2)
R_{merge} (%)	8.0 (44.0)
Refinement	
resolution (Å)	48.00−1.50
no. of reflections	19091
R_{factor} (%), R_{free}	0.149, 0.166
no. of protein atoms	255
no. of solvent atoms	58
mean B-value (Å^2)	12.845
rmsd bond lengths (Å)	0.011
rmsd bond angles (deg)	1.546
Ramachandran plot	
most favored (%)	96.3
additionally allowed (%)	3.7

followed by one wash in ice-cold 100% ethanol. After drying, the acid-insoluble radioactivity on the filter papers was measured using a scintillation counter. The molar amount of incorporated biotin was predicted by multiplying the measured counts per minutes by total assay biotin concentration/counts of total sample. Values for K_m and k_{cat} were determined by fitting a plot of rate (micromolar incorporated biotin per second per micromolar HCS or BirA) versus substrate concentration to the Michaelis−Menten equation or to a sigmoid model using GraphPad Prism (GraphPad Software Inc., San Diego, CA).

p-67L Crystallization. Wild-type p-67L crystals were grown by vapor diffusion at 20 °C in a sitting drop, mixing 100 nL of protein (21 mg/mL) and 50 nL of mother liquor consisting of 20% (v/v) PEG3350 and 0.2 M sodium formate. Well-diffracting crystals appeared after 21 days and reached a maximum size of 0.2 mm. Crystals were also obtained with chymotrypsin treatment (Roche) prior to crystal screen setup, with a protease-to-protein ratio of 1:1000. Two crystal morphologies were observed: diamond-shaped crystals grown in 0.1 M MMT buffer (1:2:2 DL-malic acid:MES:Tris base) and 30% (v/v) PEG1K (pH 7.0) and obelisk-shaped crystals grown in 30% (v/v) jeff2001 and 0.1 M HEPES, pH 7.0. All crystals were cryoprotected in mother liquor supplemented with 20% ethylene glycol and flash frozen in liquid nitrogen.

Data Collection. Diffraction data to 1.5 Å resolution were collected at beamline X10SA of the Swiss Light Source (Villigen, Switzerland). Data were processed using MOSFLM (*21*) and SCALA from the CCP4 program suite (*22*). p-67L crystals belonged to the hexagonal space group $P6_422$ (Table1). The structure was determined by molecular replacement using the program PHASER (*23*) and the unbiotinylated BCC domain from *Pyrococcus horikoshii* as search model (*Ph*BCCPΔN76, PDB code 2D5D). Initial phases were generated from a clear molecular replacement solution. Automated model building was performed using ARP/wARP (*24*), followed by several rounds of iterative manual model building and REFMAC refinement (*25*). Coordinates and structure factors for the final model, which consisted of one truncated polypeptide chain (residues 3−37) in the asymmetric unit, were deposited in the Protein Data Bank with the accession code 2JKU.

RESULTS

HCS Has Reduced Activity toward BCCP87. Biotinylation assays comparing recombinant human (HCS) and bacterial (BirA) BPL acting on (human) p-67 versus (bacterial) BCCP87 were conducted using two different assays of biotin attachment. The first assay assessed the incorporation of radiolabeled biotin ([^{14}C]biotin) into the acceptor peptide using electrophoresis and autoradiography to detect the radiolabeled product (Figure 2A). After 1 h incubation at 20 °C, BirA labeled p-67 and BCCP87 to the same extent (Figure 2A (i), "+BirA"). On the other hand, HCS labeled p-67 to saturation but labeled BCCP87 only weakly (Figure 2A (i), "+HCS"), and it remained incompletely biotinylated even after 2 h (compare (i) and (ii)). As many previous reports described biotinylation assays at 30−37 °C for optimal biotinylation conditions, the assay was repeated with HCS at 37 °C (Figure 2A (iii)). While BCCP87 was labeled by HCS to a greater extent at 37 °C compared to 20 °C, the level was still much lower than when BirA was used, confirming that the bacterial protein is a poor substrate for HCS.

The kinetic parameters for biotin addition to BCCP87 or p-67 by each biotin ligase were determined at 37 °C by varying the concentration of apoprotein substrate (Figure 2B (i)−(iv), Table 2). The data for BirA with BCCP87 are found to be within the range of previously reported values (*13*). These values show that each enzyme biotinylates its native substrate with similar efficiency (k_{cat}/K_m, Table 2). Interestingly, while BirA shows a specificity toward p-67 which is comparable to that for its own substrate, HCS demonstrates a 20-fold reduction in k_{cat}/K_m when using BCCP87 as a substrate. This decrease in reaction efficiency is due to a 6-fold increase in K_m and 3-fold decrease in rate, when compared with p-67. These observations fit with those made using the first biotinylation assay, indicating that HCS does not interact as readily with BCCP87 as with p-67.

p-67 Crystallization Requires in Situ Proteolysis. The above results suggested that a structural difference between BCCP87 and p-67 prevented an optimal interaction and catalysis of HCS with BCCP87 and, hence, a weak biotinylation reaction. We therefore determined the crystal structure of p-67 for comparison with the known structure of BCCP87.

Crystals were obtained only with the longer contruct of p-67 (p-67L), after 1 month incubation in nanoliter drops where fungal growth was observed (Figure 3A). These crystals diffracted X-rays to high resolution (1.4 Å).

The homologous *Ph*BCCPΔN76 structure (40% sequence identity) was used to generate phases by molecular replacement in an initial attempt to build a full-length model of p-67L (residues 3−72). However, refinement of this model resulted in unusually high R and R_{free} values (> 0.4) which was unexpected considering the structural homology and the high resolution of the data (1.4 Å). Examination of the $F_o - F_c$ difference density map did not indicate any additional ligands that required fitting. The high-resolution electron density map confirmed that residues 3−37 were built correctly for one chain (chain A) followed by a clear chain break, indicating that the β-hairpin loop was not resolved. A close inspection of the map further revealed that the density following the chain break corresponded not to the

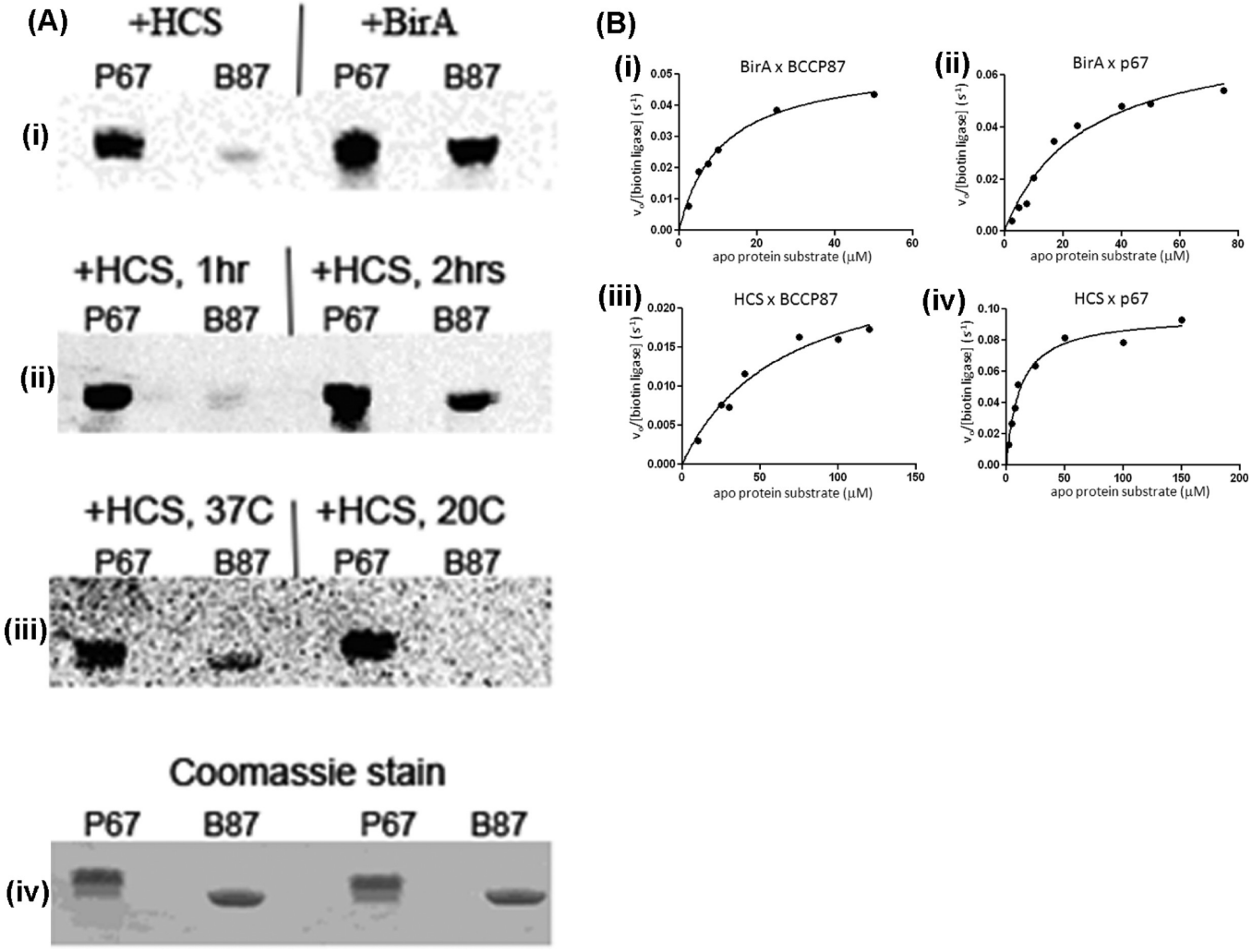

FIGURE 2: Biotinylation of p-67 and BCCP87 by BirA and HCS. (A) Autoradiography of [^{14}C]biotin attachment to BCCP87 (B87) and p-67 by BirA or HCS resolved by SDS−PAGE. (i) HCS versus BirA, with incubations for 1 h at 20 °C. (ii) HCS only, with incubations at 20 °C for 1 versus 2 h. (iii) HCS only, with incubations for 1 h at 37 versus 20 °C. (iv) Coomassie Blue-stained gel showing equal loading of BCCP87 and p-67. (B) Steady-state kinetic analyses of HCS and BirA as a function of apoprotein substrate (p-67, BCCP87) are shown. In each plot, the line represents nonlinear regression to the Michaelis−Menten equation.

Table 2: Kinetic Constants for the BirA- and HCS-Catalyzed Reaction

biotin ligase	protein substrate	K_m (μM)	k_{cat} (s^{-1})	k_{cat}/K_m ($\times 10^4$ M^{-1} s^{-1})
BirA	BCCP87	10.8 ± 1.4	0.054 ± 0.002	0.50
BirA	p-67	26.7 ± 6.4	0.077 ± 0.008	0.29
HCS	BCCP87	64.9 ± 18	0.028 ± 0.0004	0.043
HCS	p-67	11.4 ± 1.9	0.096 ± 0.005	0.84

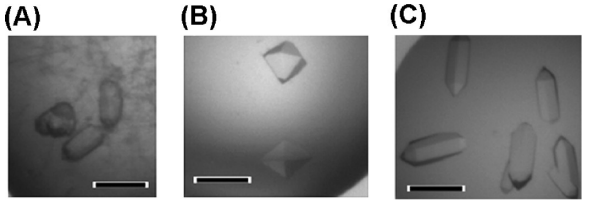

FIGURE 3: Crystals of (A) wild-type p-67L in nanoliter drops contaminated with fungal growth and (B, C) wild-type p-67 following *in situ* proteolysis using chymotrypsin at 1:1000 vs p67 L. Scale bars are 0.15 mm in length.

C-terminal half of p-67L but instead to an additional copy of the N-terminal half encompassing residues 3−37 (chain B) (Figure 4A). Chain B packed with chain A to form a complete pseudo-β-sandwich fold (Figure 4B) analogous to the structures previously reported for full-length BCC, such as *Ph*BCCPΔN76 (Figure 4C). The absence of the protruding thumb loop in p-67L was confirmed by comparing it with the structure of BCCP87, where the thumb loop resides in the region connecting strands β2 and β3 (Figure 4D). A thumb loop or similar structure was not observed in the p-67L structure determined in this study.

The above observations suggested that *in situ* proteolysis may have occurred during the course of crystallization, with the solvent-exposed β-hairpin loop the likely site of proteolysis. This was supported by two lines of evidence: (a) the crystal asymmetric unit could only accommodate the content of a full-length p-67L or two half-p-67L molecules and (b) contaminating fungus was observed in drops that yielded p-67L crystals, providing the likely

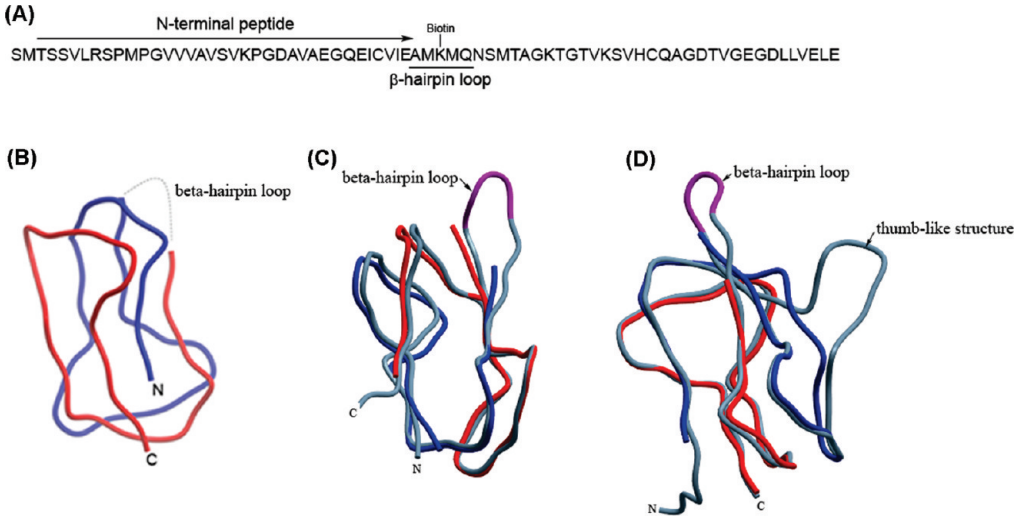

FIGURE 4: Backbone structure of *in situ* proteolytically digested p-67 (2KJU). A single chain (chain A in red, residues 3−37) forms an antiparallel dimer with itself (chain B in blue), forming a β-sandwich fold. (A) Sequence of p-67, indicating the N-terminal half (residues 3−37) and the β-hairpin loop. (B) The truncated structure of p-67 with N- and C-terminal ends of each chain labeled. Chains A and B are colored red and blue, respectively. The β-hairpin loop, which was removed by digestion, is indicated with a broken line. (C) Superposition of truncated p-67 and full-length *Ph*BCCPΔN76 (2EVB) from *P. horikoshii* (in gray). The missing β-hairpin loop in p-67 is highlighted in purple. N- and C-termini are indicated. The two structures are highly similar (rmsd = 0.381 Å). (D) Superposition of truncated p-67 with full-length BCCP87 (1BDO, in gray). A thumb-like loop, found between β-strands 2 and 3 in BCCP87, is not found in p-67. Structure manipulation was conducted with Molsoft ICM-Browser (La Jolla, CA).

source of a protease(s) that targeted the β-hairpin loop which otherwise hindered crystallization. Serendipitous proteolysis from fungal proteases has been reported previously in crystallization studies (*26*). To consider this possibility, crystallization was set up with limiting amounts of chymotrypsin (1:1000). This procedure reportedly improves the likelihood of protein crystallization, possibly by removing highly disordered regions that would hinder crystal packing (*27*). Two crystal forms of p-67L (diamond- and obelisk-shaped) appeared after 1 day (Figure 3B,C). Both forms diffracted data to high resolution and resulted in the same truncated p-67L structure (residues 3−37) as observed above (data not shown).

HCS Can Biotinylate Thumbless BCCP87 (BCCPΔT). As the protruding thumb loop in BCCP87 is predicted to interfere with the activity of HCS, we speculated that a thumbless BCCP87 would show recovered biotinylation by the human enzyme. To test this conjecture, BCCP87 without the thumb loop was expressed and assayed in the same manner as for BCCP87. The construct, BCCP87ΔT, was generated by replacing the seven residues constituting the thumb loop (TPSPDAK) with a single alanine residue, which was proposed by molecular modeling to relieve an unfavored Ramachandran angle (*20*). This construct was also shown to be biotinylated by BirA at the same rate as wild-type BCCP87, indicating that this deletion does not compromise the interaction with BirA (*20*, *28*). When BCCP87ΔT was the substrate for HCS-catalyzed transfer of [^{14}C]biotin, the reaction proceeded to a similar extent as for p-67, following 30 and 60 min incubation (Figure 5A). The analysis of kinetic parameters for HCS with BCCP87ΔT resulted in a severalfold improvement in apparent affinity. Unexpectedly, the plot of reaction velocity versus substrate concentration (Figure 5B (i)) produced a sigmoid profile akin to an allosteric effect (see Discussion).The $S_{0.5}$, representing an estimate of the substrate concentration at half-maximal velocity (*29*), was found to be 10−15 μM. To the extent that this relates to K_m, the value indicates a restored affinity approaching that of the wild-type substrate. As well, the k_{cat} of this reaction was predicted at 0.060 ±0.00097, s^{-1}, which also suggests restoration toward wild-type activity. A similar sigmoid profile was observed when BirA was used as the enzyme, showing a k_{cat} predicted at 0.068 ±0.0013, s^{-1}, although its $S_{0.5}$ was in the vicinity of 25−30 μM (Figure 5B (ii)). These results indicate that the poor reaction using the autoradiography assay was in large part due to the poor affinity of the BCCP87 substrate with HCS so that at the assay concentration of 100 μM BCCP87, the substrate was not saturating. Deletion of the thumb loop in BCCP87 increased the affinity of the substrate sufficiently to reach saturation under conditions of the assay.

DISCUSSION

Biotin-attachment domains are recognized and modified by biotin protein ligases from different species. Yet, in this study, we found that while BirA could biotinylate its cognate BCCP and human p-67 at similar rates, human HCS had little activity toward BCCP87. Sequence comparison suggesting that p-67 differs from BCCP87 in lacking a putative protruding thumb loop was confirmed by determination of the three-dimensional structure of p-67L. Significantly, we showed that HCS is active toward BCCPΔT lacking the protruding thumb. Our data provide a molecular basis for the difference in specificity between the human and bacterial BPL. We conclude that the presence of the protruding thumb loop in BCCP87 reduces its interaction with HCS.

Unexpectedly, the structure of p67 was comprised of two N-terminal halves of the protein which were packed to form a complete pseudo-β-sandwich fold, demonstrating remarkable similarity to full-length *Ph*BCCPΔN76 on superimposing the two structures (Figure 4C). Indeed, the similarity of the domains flanking the biotin-attachment site has been noted previously (*30*). Alignment of the N- and C-terminal halves of the protein demonstrates the identity or similarity of key residues and the precise correspondence of their β strands. Our results lend support to the notion of sequence duplication as the origin of the 2-fold symmetry defining the two halves of the protein.

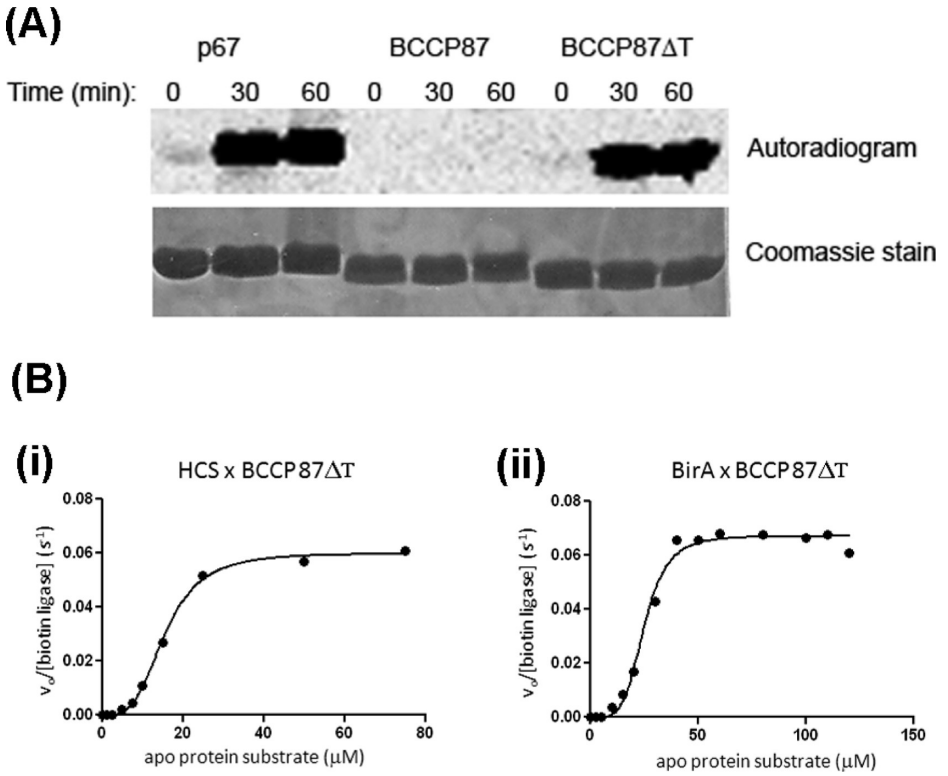

FIGURE 5: Biotinylation of BCCP87ΔT by HCS. (A) HCS attachment of [^{14}C]biotin on p-67, BCCP87, and BCCP87ΔT was analyzed over time at 20 °C. Top panel: Autoradiography of reaction products for the indicated times. Bottom panel: Gel stained with Coomassie Blue showing equal loading of each substrate. (B) Steady-state kinetic analysis of HCS and BirA as a function of BCCP87ΔT. The line represents nonlinear regression to the allosteric sigmoidal equation.

The odd behavior of the kinetic data shifting toward a sigmoid profile when assaying the mutant but not wild-type BCCP87 as substrate for HCS and BirA indicates a unique behavior of the mutant substrate in the biotinylation reaction. The plot implies a cooperative behavior of the assay. HCS has been shown to be a monomer in solution, including when complexed with 5′-biotinyl-AMP, the substrate of the biotin transfer reaction (*31*). Wild-type BCCP87 also behaves as a monomer under conditions of catalysis (*10*, *13*). On the other hand, several mutant forms of BCCP87 containing single amino acid substitutions were shown to behave as dimers by mass spectroscopy. Further, *E. coli* expressing a full-length, temperature-sensitive BCCP could be complemented partially by a mutant BCCP lacking a biotin acceptor site, providing *in vivo* evidence of the productive interaction of mutant polypeptides with dissimilar mutations (*13*, *20*). Along these lines, we speculate that increasing concentrations of BCCP87ΔT promoted protective polypeptide associations, with resulting improved interaction with either biotin protein ligase and a consequent sigmoid velocity profile. The effect is pronounced. The Hill coefficient for BirA with BCCP87 is 1.2 ± 0.2, while for HCS with p67 it is 1.1 ± 0.3, both indicating absence of cooperativity. When the protein substrate was tested with the biotin ligase of the other species, cooperative effects could be seen. BirA with p67 gave a Hill coefficient of 1.8 ± 0.2, and HCS with BCCP87 gave 2.9 ± 0.6. Significantly, when the mutant BCCP87ΔT substrate was used, the Hill coefficient became far more pronounced, reaching 4.5 ± 0.4 for BirA and 5.6 ± 1.4 for HCS. It is difficult to escape the notion that the protein substrate produces adventitious self-associations either free in solution or on binding the biotin ligase, as originally demonstrated for the BCCP87 point mutations (*13*, *20*). Whatever the mechanism, the resulting substrate concentration at half-maximal velocity, $S_{0.5}$, was much reduced compared to the K_M obtained for HCS acting on wild-type BCCP87. Indeed, the affinity of the thumbless protein for HCS appeared to improve to the wild-type range, providing a simple explanation for the dramatic improvement in activity using the autoradiography protocol. Interestingly, the $S_{0.5}$ predicted for BirA acting on BCCP87ΔT (25−30 μM) was similar to the K_M obtained for BirA with p-67 (27 μM), indicating that, notwithstanding its apparent oligomeric state, BCCP87ΔT may resemble p67 and interact with BirA in a similar manner.

Alignment of BCCP87 with BCC domains from various organisms suggests a clear location for the thumb loop (Figure 6 (*27*)). A high level of conservation before and after the thumb loop sequence is observed and allows for its detection. Species with a seven residue gap in the sequence alignment are presumed not to have a thumb loop, thereby delineating "boundaries" for the thumb loop. The sequence immediately N-terminal to the gap tends to be conserved (GKLIR/Q) and differs from the sequence when a thumb loop is present (GTFYRS/T) (Figure 6). Second, the seven residue thumb loop contains an invariant proline at its center. In BCCP87, this proline is located at the tip end of a β turn in the loop. Curiously, the thumb loop is predicted only in bacterial and some plant plastidal ACCs.

Recently, a complex crystal structure of BPL and BCCP from *P. horikoshii* was reported, which visualized the spatial relationship between BPL and BCCP in the enzyme−substrate complex (*32*). While BCCP from *P. horikoshii* does not contain the protruding thumb (Figure 1), this structure indicates the possibility of steric clash with the protruding thumb in BCCP87 through association with BPL. These structural data lend support to the observations of a reduced affinity between HCS and BCCP87. The association between HCS and its protein substrate is anticipated to resemble this complex. A complex structure

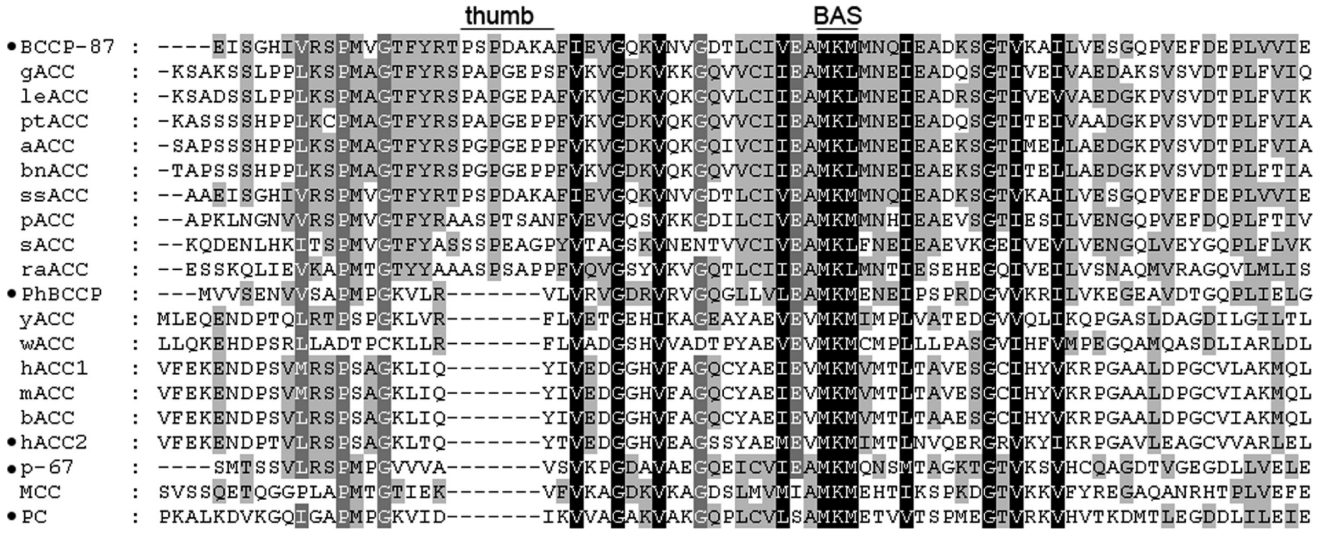

FIGURE 6: Sequence alignment of BCC domains predicting the presence or absence of the loop region. Domains with structural data are indicated with a bullet. The thumb region and biotin-attachment site (BAS) are indicated. The aligned sequences are as follows: *E. coli* BCCP87 (BCCP-87), soybean ACC (gACC), tomato ACC (leACC), cottonwood ACC (ptACC), *A. thaliana* ACC-2 (aACC), rape ACC (bnACC), *S. sonnei* ACC (ssACC), *P. aeruginosa* ACC (pACC), *B. subtilis* ACC (sACC), *C. merolae* (raACC), *P. horikoshii* ACC (*Ph*BCCP), *S. pombe* ACC (yACC), wheat ACC (wACC), human ACC-1 (hACC1), human ACC-2 (hACC2), bovine ACC (bACC), mouse ACC (mACC), p-67, human MCC (hMCC), and human PC (hPC).

between BirA and BCCP87 has yet to be resolved, which would define the structural differences in BirA that accommodate the protruding thumb loop.

The function of the protruding thumb loop in BCCP87 and why it is not required in other thumbless carboxylases are unclear. Deletion of the thumb loop in full-length *E. coli* BCCP resulted in a reduction in fatty acid synthesis, with a failure to complement a BCCP temperature-sensitive mutant strain in *E. coli* (*20*). Biotinylation of this "thumbless" BCCP mutant was, however, unaltered. It appears, therefore, that the thumb loop is essential for fatty acid synthesis and therefore bacterial viability, but it is not associated with the catalytic specificity of BirA. There is no parallel in mammalian cells, so our finding relates to the structure of the biotin-attachment domain rather than differentiating biological specificity, despite the activity of HCS toward multiple carboxylases.

ACKNOWLEDGMENT

The authors thank Frank von Delft and members of the crystallography group of the Structural Genomics Consortium for assistance with X-ray data collection, completed during a training visit by S.H. to the SGC at Oxford University, John E. Cronan (University of Illinois) for providing reagents, Dongxin Jia (University of Calgary) for assistance with kinetic analysis, and D. Beckett (University of Maryland, College Park) for hosting S.H. in her laboratory and providing specialized reagents. This work is based on diffraction data collected at beamline PXII of the Swiss Light Source, Paul Scherrer Institute, Villigen, Switzerland.

REFERENCES

1. Lamhonwah, A. M., Barankiewicz, T. J., Willard, H. F., Mahuran, D. J., Quan, F., and Gravel, R. A. (1986) Isolation of cDNA clones coding for the alpha and beta chains of human propionyl-CoA carboxylase: chromosomal assignments and DNA polymorphisms associated with PCCA and PCCB genes. *Proc. Natl. Acad. Sci. U.S.A. 83*, 4864–4868.
2. Kalousek, F., Darigo, M. D., and Rosenberg, L. E. (1980) Isolation and characterization of propionyl-CoA carboxylase from normal human liver. Evidence for a protomeric tetramer of nonidentical subunits. *J. Biol. Chem. 255*, 60–65.
3. Lamhonwah, A. M., Quan, F., and Gravel, R. A. (1987) Sequence homology around the biotin-binding site of human propionyl-CoA carboxylase and pyruvate carboxylase. *Arch. Biochem. Biophys. 254*, 631–636.
4. Chapman-Smith, A., and Cronan, J. E., Jr. (1999) The enzymatic biotinylation of proteins: a post-translational modification of exceptional specificity. *Trends Biochem. Sci. 24*, 359–363.
5. León-Del-Rio, A., Leclerc, D., Akerman, B., Wakamatsu, N., and Gravel, R. A. (1995) Isolation of a cDNA encoding human holocarboxylase synthetase by functional complementation of a biotin auxotroph of *Escherichia coli*. *Proc. Natl. Acad. Sci. U.S.A. 92*, 4626–4630.
6. Barker, D. F., and Campbell, A. M. (1981) The birA gene of *Escherichia coli* encodes a biotin holoenzyme synthetase. *J. Mol. Biol. 146*, 451–467.
7. Leon-Del-Rio, A., and Gravel, R. A. (1994) Sequence requirements for the biotinylation of carboxyl-terminal fragments of human propionyl-CoA carboxylase alpha subunit expressed in *Escherichia coli*. *J. Biol. Chem. 269*, 22964–22968.
8. Chapman-Smith, A., Turner, D. L., Cronan, J. E., Jr., Morris, T. W., and Wallace, J. C. (1994) Expression, biotinylation and purification of a biotin-domain peptide from the biotin carboxy carrier protein of *Escherichia coli* acetyl-CoA carboxylase. *Biochem. J. 302*, 881–887.
9. Li, S. J., and Cronan, J. E., Jr. (1992) The gene encoding the biotin carboxylase subunit of *Escherichia coli* acetyl-CoA carboxylase. *J. Biol. Chem. 267*, 855–863.
10. Nenortas, E., and Beckett, D. (1996) Purification and characterization of intact and truncated forms of the *Escherichia coli* biotin carboxyl carrier subunit of acetyl-CoA carboxylase. *J. Biol. Chem. 271*, 7559–7567.
11. Yao, X., Wei, D., Soden, C., Jr., Summers, M. F., and Beckett, D. (1997) Structure of the carboxy-terminal fragment of the apo-biotin carboxyl carrier subunit of *Escherichia coli* acetyl-CoA carboxylase. *Biochemistry 36*, 15089–15100.
12. Athappilly, F. K., and Hendrickson, W. A. (1995) Structure of the biotinyl domain of acetyl-coenzyme A carboxylase determined by MAD phasing. *Structure 3*, 1407–1419.
13. Chapman-Smith, A., Morris, T. W., Wallace, J. C., and Cronan, J. E., Jr. (1999) Molecular recognition in a post-translational modification of exceptional specificity. Mutants of the biotinylated domain of acetyl-CoA carboxylase defective in recognition by biotin protein ligase. *J. Biol. Chem. 274*, 1449–1457.
14. Reddy, D. V., Rothemund, S., Shenoy, B. C., Carey, P. R., and Sönnichsen, F. D. (1998) Structural characterization of the entire 1.3S subunit of transcarboxylase from *Propionibacterium shermanii*. *Protein Sci. 7*, 2156–2163.
15. Bagautdinov, B., Matsuura, Y., Bagautdinova, S., and Kunishima, N. (2007) Crystallization and preliminary X-ray crystallographic studies of the biotin carboxyl carrier protein and biotin protein ligase complex

from *Pyrococcus horikoshii* OT3. *Acta Crystallogr., Sect. F: Struct. Biol. Cryst. Commun. 63*, 334–337.
16. Xiang, S., and Tong, L. (2008) Crystal structures of human and Staphylococcus aureus pyruvate carboxylase and molecular insights into the carboxyltransfer reaction. *Nat. Struct. Mol. Biol. 15*, 295–302.
17. Lee, C. K., Cheong, H. K., Ryu, K. S., Lee, J. I., Lee, W., Jeon, Y. H., and Cheong, C. (2008) Biotinoyl domain of human acetyl-CoA carboxylase: structural insights into the carboxyl transfer mechanism. *Proteins 72*, 613–624.
18. Polyak, S. W., Chapman-Smith, A., Mulhern, T. D., Cronan, J. E., Jr., and Wallace, J. C. (2001) Mutational analysis of protein substrate presentation in the post-translational attachment of biotin to biotin domains. *J. Biol. Chem. 276*, 3037–3045.
19. Healy, S., Heightman, T. D., Hohmann, L., Schriemer, D., and Gravel, R. A. (2009) Nonenzymatic biotinylation of histone H2A. *Protein Sci. 18*, 314–328.
20. Cronan, J. E., Jr. (2001) The biotinyl domain of *Escherichia coli* acetyl-CoA carboxylase. Evidence that the "thumb" structure is essential and that the domain functions as a dimer. *J. Biol. Chem. 276*, 37355–37364.
21. Leslie, A. G. (1999) Integration of macromolecular diffraction data. *Acta Crystallogr., Sect. D: Biol. Crystallogr. 55*, 1696–1702.
22. Collaborative Computational Project, Number 4 (1994) The CCP4 suite: programs for protein crystallography. *Acta Crystallogr., Sect. D: Biol. Crystallogr. 50*, 760–763.
23. McCoy, A. J. (2007) Solving structures of protein complexes by molecular replacement with Phaser. *Acta Crystallogr., Sect. D: Biol. Crystallogr. 63*, 32–41.
24. Perrakis, A., Harkiolaki, M., Wilson, K. S., and Lamzin, V. S (2001) ARP/wARP and molecular replacement. *Acta Crystallogr., Sect. D: Biol. Crystallogr. 57*, 1445–1450.
25. Murshudov, G. N., Vagin, A. A., Lebedev, A., Wilson, K. S., and Dodson, E. J. (1999) Efficient anisotropic refinement of macromolecular structures using FFT. *Acta Crystallogr., Sect. D: Biol. Crystallogr. 55*, 247–255.
26. Mandel, C. R., Gebauer, D., Zhang, H., and Tong, L. (2006) A serendipitous discovery that in situ proteolysis is essential for the crystallization of yeast CPSF-100 (Ydh1p). *Acta Crystallogr., Sect. F: Struct. Biol. Cryst. Commun. 62*, 1041–1045.
27. Midwest Center for Structural Genomics, Structural Genomics Consortium (2007) In situ proteolysis for protein crystallization and structure determination. *Nat. Methods 4*, 1019–1021.
28. Reche, P., and Perham, R. N. (1999) Structure and selectivity in post-translational modification: attaching the biotinyl-lysine and lipoyl-lysine swinging arms in multifunctional enzymes. *EMBO J. 18*, 2673–2682.
29. Palmer, T. (1995) Understanding Enzymes, 4th ed., Ellis Horwood Ltd., London.
30. Toh, H., Kondo, H., and Tanabe, T. (1993) Molecular evolution of biotin-dependent carboxylases. *Eur. J. Biochem. 215*, 687–696.
31. Ingaramo, M., and Beckett, D. (2009) Distinct amino termini of two human HCS isoforms influence biotin acceptor substrate recognition. *J. Biol. Chem. 284*, 30862–30870.
32. Bagautdinov, B., Matsuura, Y., Bagautdinova, S., and Kunishima, N. (2008) Protein biotinylation visualized by a complex structure of biotin protein ligase with substrate. *J. Biol. Chem. 283*, 14739–14750.